Available online at www.sciencedirect.com
SCIENCE DIRECT®
Journal of Power Sources 146 (2005) 237–240
JOURNAL OF POWER SOURCES
www.elsevier.com/locate/jpowsour

Structural and electrochemical study of Li–Al–Mn–O–F spinel material for lithium secondary batteries

Y.-J. Kang, J.-H. Kim, Y.-K. Sun *

Department of Chemical Engineering, Hanyang University, Seungdong-Gu, Seoul 133-791, South Korea

Available online 26 April 2005

Abstract

The structural and electrochemical properties of various Li–Al–Mn–O–F spinels were studied. $Li[Li_xAl_yMn_{2-x-y}]O_{4-z}F_z$ ($x = 0$, 0.05, $y = 0$, 0.1, $0 \le z \le 0.2$) spinels were synthesized by a solid-state reaction method. Fluorine substitution in $Li[Li_xAl_yMn_{2-x-y}]O_{4-z}F_z$ led to well-developed crystallization with octahedral morphology. In addition, $Li[Li_xAl_yMn_{2-x-y}]O_{4-z}F_z$ showed superior cycling performance and better thermal stability than $LiMn_2O_4$ and $LiAl_{0.1}Mn_{1.9}O_4$. Fluorine substitution also suppressed Mn dissolution which led to stable cycling performance at 55 °C. The differential scanning calorimetry (DSC) results showed that the anion (F for O) and cation (Li, Al for Mn) substituted spinel had better thermal stability than $LiMn_2O_4$, $Li[Al_yMn_{2-y}]O_4$, or $Li[Li_xAl_yMn_{2-x-y}]O_4$.

Keywords: $LiMn_2O_4$; Spinel; Cathode material; Al doping; F doping

1. Introduction

$LiMn_2O_4$ has been studied extensively as a cathode material for lithium rechargeable batteries because of its low cost, low toxicity and relatively elevated energy density [1–3]. Despite such advantages, significant capacity fading during cycling, especially at elevated temperatures, has frustrated the commercial use of the $LiMn_2O_4$. Although the origin of the poor cycling performance has not been fully understood, several possible mechanisms have been suggested, such as Jahn–Teller distortion [4,5], Mn dissolution at elevated temperature originating from $Mn^{3+/4+}$ redox [6,7] and changes in the crystal lattice arrangement during cycling [8].

To overcome the problem of poor cycling performance at elevated temperature, many studies have focused on cation substituted $LiMn_{2-x}M_xO_4$ (M = Al, Mg, Ni, Co, Cr, etc.). Some of these substituted spinel showed improved electrochemical performance at elevated temperature [9–12]. Another work by Sun et al. [13] and Amatucci et al. [14,15] with anion doped spinels has shown that anion doped spinels exhibit stable cyclability at elevated temperatures. Among these anion doped spinels, the two-fold substituted $LiAl_yMn_{2-y}O_{4-z}F_z$ showed improved electrochemical performance due to the combined positive effects of the retention of small lattice parameters by Al substitution and reduced average Mn oxidation state by F substitution [15,16]. The other work to improve the poor capacity and cyclability in the 4 V region of $LiMn_2O_4$, monovalent Li doping on 16d sites were also performed [4,17–20]. Because Li^+ provides a larger valence difference relative to Mn than divalent or trivalent cations, only a small amount of dopant was effective [20].

This study focused on the Li–Al substitution for Mn (16d sites) and F substitution for O (32e sites) in $LiMn_2O_4$. $Li[Li_xAl_yMn_{2-x-y}]O_{4-z}F_z$ ($x = 0$, 0.05, $y = 0$, 0.1, $0 \le z \le 0.2$) spinels were synthesized by a solid–state reaction method, and their structure, electrochemical properties and thermal properties were examined.

2. Experimental

$Li[Li_xAl_yMn_{2-x-y}]O_{4-z}F_z$ ($x = 0$, 0.05, $y = 0$, 0.1, $0 \le z \le 0.2$) spinels were synthesized using LiOH, Mn_3O_4, $Al(OH)_3$ and LiF by a solid state method. The mixture of starting materials was precalcined at 470 and 530 °C for 5 h

* Corresponding author. Tel.: +82 2 2290 0524; fax: +82 2 2282 7329.
E-mail address: yksun@hanyang.ac.kr (Y.-K. Sun).

0378-7753/$ – see front matter © 2005 Elsevier B.V. All rights reserved.
doi:10.1016/j.jpowsour.2005.03.037

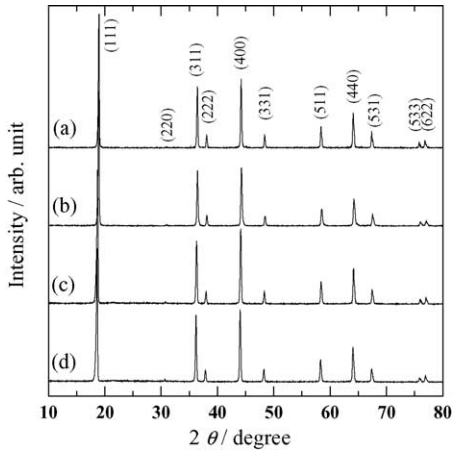

Fig. 1. X-ray diffraction patterns of $Li[Li_xAl_yMn_{2-x-y}]O_{4-z}F_z$ powders: (a) $x=0$, $y=0$, $z=0$; (b) $x=0$, $y=0.1$, $z=0$; (c) $x=0.05$, $y=0.1$, $z=0$; and (d) $x=0.05$, $y=0.1$, $z=0.2$.

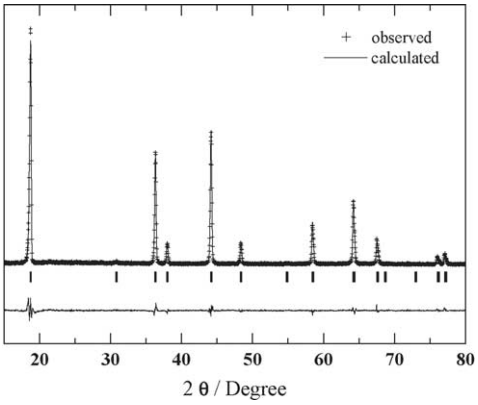

Fig. 2. Rietveld refinement profiles of XRD data for $Li_{1.05}Al_{0.1}Mn_{1.85}O_4$. Scanning electron micrographs for $Li[Li_xAl_yMn_{2-x-y}]O_{4-z}F_z$ powders: (a) $x=0$, $y=0$, $z=0$; (b) $x=0$, $y=0.1$, $z=0$; (c) $x=0.05$, $y=0.1$, $z=0$; and (d) $x=0.05$, $y=0.1$, $z=0.1$.

in O_2, respectively, and then post-calcined at 850 °C for 20 h in air.

Powder X-ray diffraction (XRD, Rint-2000, Rigaku, Japan) using a Cu Kα radiation was employed to identify the crystalline phase of the synthesized material. The collected intensity data of the XRD patterns were analyzed by the Rietveld refinement program, *Fullprof* 2000 [21]. The thermal stability of the sample was studied using differential scanning calorimetry (DSC, NETZSCH-TA4, Germany). DSC scans were conducted at a ramp rate of 2 °C min^{-1} from 50 to 350 °C. Galvanostatic charge/discharge cycling was performed in a 2032-type coin cell. For the fabrication of the positive electrode, 20 mg cathode active materials was mixed with 5 mg of conductive binder (3.33 mg of teflonized acetylene black and 1.67 mg of graphite). The mixture was pressed on 200 mm^2 stainless steel mesh current collector and dried at 130 °C for 5 h in a vacuum oven. Lithium foil was used as the negative electrode. The electrolyte solution was 1 M LiPF6 in a mixture of ethylene carbonate (EC) and diethyl carbonate (DEC) in a 1:1 volume ratio (Merck, Germany). The cell was assembled in an argon-filled glove box. To investigate the manganese dissolution during capacity fading, the amount of manganese concentration in the electrolyte solution was measured. After charging to 4.3 V, Li/$Li[Li_xAl_yMn_{2-x-y}]O_{4-z}F_z$ cells were disassembled, and the positive electrodes were immersed in a specified amount of electrolyte solution at 55 °C. The amount of dissolved manganese into the electrolyte from the cathode was determined with atomic absorption spectroscopy (Vario 6, Analyticjena, Germany).

3. Results and discussion

The powder XRD patterns of $Li[Li_xAl_yMn_{2-x-y}]O_{4-z}F_z$ ($x=0$, 0.05, $y=0$, 0.1, $0 \le z \le 0.2$) are shown in Fig. 1. All samples showed a single crystalline cubic spinel phase with a space group of $Fd\bar{3}m$ showing a homogeneous solid solution of multiple elements. From the AAS analysis, it was confirmed that the chemical compositions of the prepared powders were stoichiometric except for the anion contents which could not be determined by AAS.

The structure of $Li[Li_xAl_yMn_{2-x-y}]O_{4-z}F_z$ spinels were identified by Rietveld refinements using the $Fd\bar{3}m$ space group. The Rietveld refinement results indicated that the atoms were located in the following sites: Li atoms in 8a sites, Li, Al, Mn atoms in 16d sites, and O, F atoms in 32e sites. The Rietveld refinement patterns of $Li_{1.05}Al_{0.1}Mn_{1.85}O_4$ are shown in Fig. 2. During refinement, the sum of occupation factors for O and F anions was fixed at 1 to avoid possible refinement errors. Table 1 shows the refined results of $Li[Li_xAl_yMn_{2-x-y}]O_{4-z}F_z$. In stoichiometric $LiAl_{0.1}Mn_{1.9}O_4$, the oxidation state of Mn is +3.526, which is higher than +3.5 in $LiMn_2O_4$. For this reason, our $LiAl_{0.1}Mn_{1.9}O_4$ sample showed smaller lattice parameter than that of $LiMn_2O_4$ because of the increased amount of small Mn^{4+} ($r_{Mn^{4+}} = 0.53$ Å) and Al^{3+} ($r_{Mn^{3+}} = 0.535$ Å) ions compared to Mn^{3+} ($r_{Mn^{3+}} = 0.645$ Å) [22]. Also, $Li_{1.05}Al_{0.1}Mn_{1.85}O_4$ with the Mn oxidation state of +3.595 had a smaller lattice parameter of 8.2011 than that of $LiMn_2O_4$ and $LiAl_{0.1}Mn_{1.9}O_4$. In $Li_{1.05}Al_{0.1}Mn_{1.85}O_{4-z}F_z$, where F was substituted for O, lattice parameters increased depending on F contents due to the decreasing oxidation state of Mn. This suggests that F ions were successfully substituted

Table 1
Rietveld refinement results for $Li[Li_xAl_yMn_{2-x-y}]O_{4-z}F_z$ based on a space group of $Fd\bar{3}m$

Sample	a (Å)	Vol. (Å^3)	R_{wp} (%)	R_{Bragg} (%)
$LiMn_2O_4$	8.2496	561.428	14.4	3.06
$LiAl_{0.1}Mn_{1.9}O_4$	8.2212	555.652	14.7	2.91
$Li_{1.05}Al_{0.1}Mn_{1.85}O_4$	8.2011	551.594	12.5	2.69
$Li_{1.05}Al_{0.1}Mn_{1.85}O_{3.95}F_{0.05}$	8.2013	551.628	12.5	2.90
$Li_{1.05}Al_{0.1}Mn_{1.85}O_{3.9}F_{0.1}$	8.2015	551.667	13.0	2.75
$Li_{1.05}Al_{0.1}Mn_{1.85}O_{3.85}F_{0.15}$	8.2024	551.847	12.4	2.58
$Li_{1.05}Al_{0.1}Mn_{1.85}O_{3.8}F_{0.2}$	8.2032	552.022	12.2	1.94

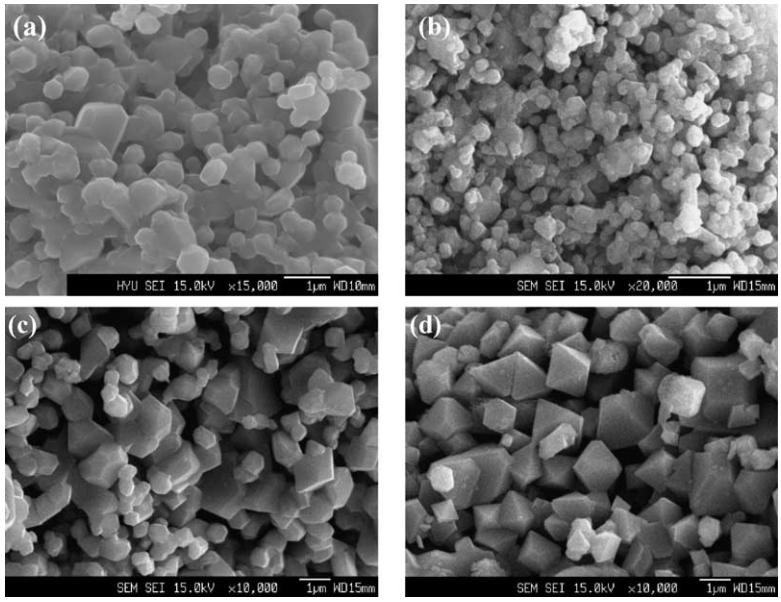

Fig. 3. Scanning electron micrographs for $Li[Li_xAl_yMn_{2-x-y}]O_{4-z}F_z$ powders: (a) $x=0$, $y=0$, $z=0$; (b) $x=0$, $y=0.1$, $z=0$; (c) $x=0.05$, $y=0.1$, $z=0$; and (d) $x=0.05$, $y=0.1$, $z=0.1$.

for O in $LiAl_{0.1}Mn_{1.9}O_4$ host structure although their quantitative amount could not be defined. Amatucci et al. [23] also observed that the substitution of oxygen by fluorine resulted in an increase in the lattice parameter and a reduction in the average Mn oxidation state.

The SEM images of $LiMn_2O_4$, $LiAl_{0.1}Mn_{1.9}O_4$, $Li_{1.05}Al_{0.1}Mn_{1.85}O_4$, and $Li_{1.05}Al_{0.1}Mn_{1.85}O_{3.9}F_{0.1}$ are shown in Fig. 3. The shape of the particles vary from spherical to cubic octahedral depending on their composition. The particle size of the $LiMn_2O_4$ and $LiAl_{0.1}Mn_{1.9}O_4$ powders are less than ~0.5 μm, and consist of irregularly polygonal shaped particles with obtuse edges. $Li_{1.05}Al_{0.1}Mn_{1.85}O_{3.9}F_{0.1}$ has an octahedral morphology with well ordered [1 1 1] direction, and consists of larger particles (1–2 μm) than $Li_{1.05}Al_{0.1}Mn_{1.85}O_4$. This result also suggests that F ions were successively substituted for O in $Li_{1.05}Al_{0.1}Mn_{1.85}O_4$ host structure.

Electrochemical properties of $Li/Li[Li_xAl_yMn_{2-x-y}]O_{4-z}F_z$ ($x=0$, 0.05, $y=0$, 0.1, $z=0$, 0.1) cells were studied at an elevated temperature of 55 °C. The operating cut-off voltages were 3.5 and 4.3 V under a constant current density of 20 mA g^{-1}. Fig. 4 shows the voltage profiles and cycling performances of the $Li/Li[Li_xAl_yMn_{2-x-y}]O_{4-z}F_z$ ($x=0$, 0.05, $y=0$, 0.1, $z=0$, 0.1) cells. The $Li/LiMn_2O_4$ cell showed the highest initial capacity of 126 mAh g^{-1} but exhibited poor cycling performance. The capacity retention of the $Li/LiAl_{0.1}Mn_{1.9}O_4$ cell was more improved than the $LiMn_2O_4$, however, it exhibited a decreased initial capacity of 117 mAh g^{-1} and significant capacity loss during cycling. For $Li/Li_{1.05}Al_{0.1}Mn_{1.9}O_4$ and $Li/Li_{1.05}Al_{0.1}Mn_{1.85}O_{3.9}F_{0.1}$ cells, their low initial capacities were offset by excellent capacity retention of 97.5% and 99.0% after 50 cycles, respectively.

Fig. 5 shows the amount of Mn dissolved from the $Li[Li_xAl_yMn_{2-x-y}]O_{4-z}F_z$ electrode into the electrolyte solution with increasing aging time. After 500 h, 198 ppm of Mn was measured in the electrolyte for $LiMn_2O_4$. For $Li_{1.05}Al_{0.1}Mn_{1.85}O_4$ electrode, significant improvement about manganese dissolution was shown. Especially, the dually substitution of anion (F for O) and cation (Li, Al for Mn) resulted in much lower amount of Mn dissolution. For $Li_{1.05}Al_{0.1}Mn_{1.85}O_{3.95}F_{0.05}$ and $Li_{1.05}Al_{0.1}Mn_{1.85}O_{3.9}F_{0.1}$, the Mn concentration in electrolyte was less than 25 ppm after 500 h even at an elevated temperature of 55 °C. Because F substitution lowers the average oxidation state of manganese, it could be thought that manganese dissolution could be facilitated by F substitution. In our $Li_{1.05}Al_{0.1}Mn_{1.85}O_{4-z}F_z$ sample ($z=0.05$ and 0.1); however, Mn dissolution was significantly suppressed by F substitution [23].

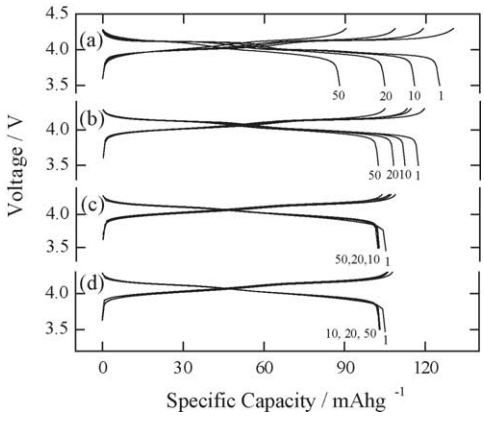

Fig. 4. Charge/discharge curves of $Li[Li_xAl_yMn_{2-x-y}]O_{4-z}F_z$ powders at 55 °C: (a) $x=0$, $y=0$, $z=0$; (b) $x=0$, $y=0.1$, $z=0$; (c) $x=0.05$, $y=0.1$, $z=0$; and (d) $x=0.05$, $y=0.1$, $z=0.1$.

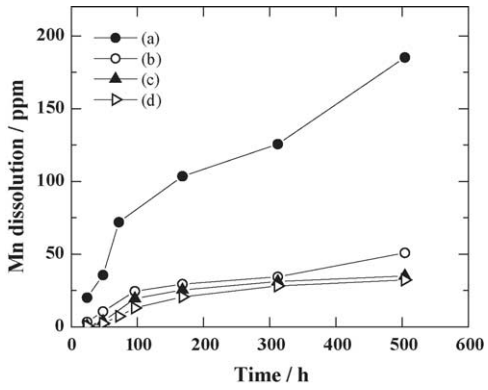

Fig. 5. Mn dissolution amount vs. storage time at 55oC of the $Li[Li_xAl_yMn_{2-x-y}]O_{4-z}F_z$ powders: (a) $x=0$, $y=0$, $z=0$; (b) $x=0.05$, $y=0.1$, $z=0$; (c) $x=0.05$, $y=0.1$, $z=0.05$; and (d) $x=0.05$, $y=0.1$, $z=0.1$.

Fig. 6 shows the DSC results for $Li[Li_xAl_yMn_{2-x-y}]O_{4-z}F_z$ ($x=0$, 0.05, $y=0$, 0.1, $0 \le z \le 0.1$) charged to 4.3 V. The onset temperature for thermal decomposition is raised significantly and the total amount of the reaction heat is reduced by Li–Al–F substitutions. For the $Li_{1.05}Al_{0.1}Mn_{1.85}O_{3.95}F_{0.05}$ charged to 4.3 V, one major peak is observed at 257 °C whereas for $LiMn_2O_4$ one peak was observed at around 240 °C. Although the positions of the exothermic peaks are similar in $Li_{1.05}Al_{0.1}Mn_{1.85}O_{4-z}F_z$ ($z=0$–0.1), the heat associated with each exothermic peak is significantly decreased with increasing fluorine content: 99.631 W g^{-1} ($z=0$), 79.489 W g^{-1} ($z=0.05$), 49.815 W g^{-1} ($z=0.1$), respectively. Though the reason is not fully understood, it is possible that well developed octahedral morphology and particle size of $Li[Li_xAl_yMn_{2-x-y}]O_{4-z}F_z$ improves the thermal stability. Jouanneau et al. [24] recently reported that thermal stability depends on morphology, which means that larger particles have greater thermal stability.

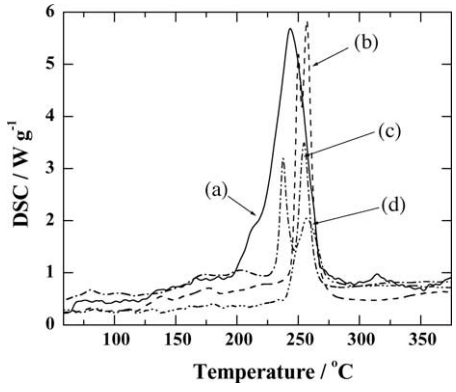

Fig. 6. DSC scans of charged $Li[Li_xAl_yMn_{2-x-y}]O_{4-z}F_z$ cathodes at 4.3 V charge cut-off. The scan rate was 2 °C min^{-1}: (a) $x=0$, $y=0$, $z=0$; (b) $x=0.05$, $y=0.1$, $z=0$; (c) $x=0.05$, $y=0.1$, $z=0.05$; and (d) $x=0.05$, $y=0.1$, $z=0.1$.

4. Conclusion

The anion and cation substituted spinel $Li[Li_xAl_yMn_{2-x-y}]O_{4-z}F_z$ ($x=0$, 0.05, $y=0$, 0.1, $0 \le z \le 0.2$) electrode showed excellent cyclability at an elevated temperature. The capacity retentions of the anion and cation substituted spinel electrode after 50th cycles at 55 °C was 99% of the initial capacity of 105 mAh g^{-1}. The excellent cyclability resulting from small Mn dissolution of the anion and cation substituted spinel show that this material is an attractive cathode material for lithium secondary batteries. DSC data showed that the anion and cation substituted spinel has better thermal stability than $LiMn_2O_4$, $Li[Al_yMn_{2-y}]O_4$, and $Li[Li_xAl_yMn_{2-x-y}]O_4$ spinels.

Acknowledgements

This work was supported by KOSEF through the Research Center for Energy Conversion and Storage.

References

[1] J.M. Tarascon, E. Wang, F.K. Shokoohi, W.R. McKinnon, S. Colson, J. Electrochem. Soc. 138 (1991) 2859.
[2] T. Ohzuku, M. Kitagawa, T. Hirayi, J. Electrochem. Soc. 137 (1990) 769.
[3] J.M. Tarascon, D. Guyomard, Electrochim. Acta 38 (1991) 1221.
[4] R.J. Gummow, A. de Kock, M.M. Thackeray, Solid State Ionics 69 (1994) 59.
[5] M.M. Thackeray, Y. Shao-Horn, A.J. Kahaian, Electrochem. Solid-State Lett. 1 (1998) 7.
[6] D.H. Jang, Y.J. Shin, S.M. Oh, J. Electrochem. Soc. 143 (1996) 2204.
[7] Y. Xia, Y. Zhou, M. Yoshio, J. Electrochem. Soc. 144 (1997) 2593.
[8] P. Arora, B.N. Popov, R.E. White, J. Electrochem. Soc. 145 (1998) 807.
[9] Y.-K. Sun, Electrochem. Commun. 3 (2001) 199.
[10] D. Song, H. Ikuta, T. Uchida, M. Wakihara, Solid State Ionics 117 (1999) 151.
[11] K. Amine, H. Tukamoto, H. Yasuda, Y. Fugita, J. Power Sources 68 (1997) 604.
[12] Q. Feng, H. Hanoh, Y. Miyai, K. Ooi, Chem. Mater. 7 (1995) 379.
[13] Y.-K. Sun, G.S. Park, Y.S. Lee, M. Yoshio, K.S. Nahm, J. Electrochem. Soc. 148 (9) (2001) A994.
[14] G.G. Amatucci, J.M. Tarascon, U.S. Pat. 5,674,645 (1997).
[15] G.G. Amatucci, A. Byylr, C. Siagala, P. Alfonse, J.M. Tarascon, Solid State Ionics 104 (1997) 13.
[16] G.G. Amatucci, N. Pereira, T. Zheng, J.M. Tarascon, J. Electrochem. Soc. 148 (2) (2001) A171.
[17] M.H. Rossouw, A. de Kock, L.A. de Picciotto, M.M. Thackeray, W.I.F. David, R.M. Ibberson, Mater. Res. Bull. 25 (1990) 173.
[18] Y. Gao, J.R. Dahn, J. Electrochem. Soc. 143 (1996) 100.
[19] Y. Xia, M. Yoshio, J. Electrochem. Soc. 144 (1997) 4186.
[20] N.V. Kosova, N.F. Uvarov, E.T. Devyatkina, E.G. Avvakumov, Solid State Ionics 135 (2000) 107.
[21] J. Rodriguez-Carjaval, Physica B 192 (1993) 55.
[22] J.A. Dean, Lange's Handbook of Chemistry, fourth ed., McGraw-Hill Inc., USA, 1992, pp. 4.13–4.17.
[23] G. Amatucci, A.Du. Pasquier, A. Blyr, Y. Zheng, J.-M. Tarascon, Electrochim. Acta 45 (1999) 255.
[24] S. Jouanneau, D.D. MacNeil, Z. Lu, S.D. Beattie, G. Murphy, J.R. Dahn, J. Electrochem. Soc. 150 (2003) A1299.